ARTICLE

Saturated Cavity Ring-Down Spectroscopy of $^{12}C^{16}O_2$ near 1.57 μm

Shan Jiang, Yan Tan, An-Wen Liu*, Xiao-Guo Zhou, Shui-Ming Hu

Department of Chemical Physics, University of Science and Technology of China, Hefei 230026, China

(Dated: Received on May 12, 2023; Accepted on June 1, 2023)

We present the saturated absorption spectroscopy of the 30012←00001 band of $^{12}C^{16}O_2$ by a comb-locked cavity ring-down spectrometer near 1.57 μm. Positions of 37 lines with rotational quantum numbers up to 68 were determined with an accuracy of a few kHz. Comparisons of the ro-vibrational energy levels determined in this work with the Doppler-limited experimental values from literature and those from the CDSD2019 databank are given. Deviations exceeding 1 MHz were observed in the transitions blended by other carbon dioxide isotopologues.

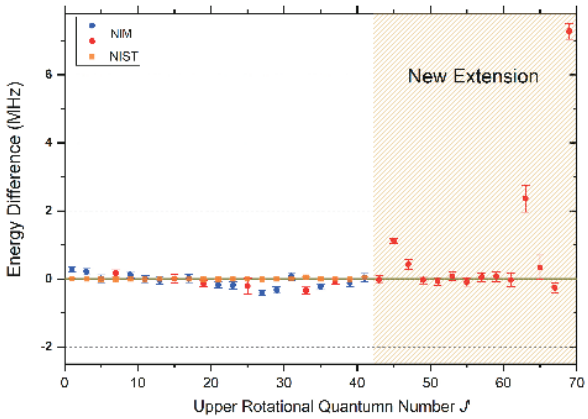

Key words: Saturated absorption spectroscopy, Cavity ring-down spectroscopy, $^{12}C^{16}O_2$, High precision

I. INTRODUCTION

Carbon dioxide (CO_2), the most important greenhouse gas, has a global average concentration of over 400 ppm, 43% increased since pre-industrial times. Numerous remote sensing tasks, such as OCO-2/3 (USA) [1, 2], GOSAT (Japan) [3], Tansat (China) [4], and TCCON (Global) [5], *etc.*, continuously monitor the atmospheric column densities to determine the long-term change. The retrieval accuracy of the column densities relies on the accuracy of the line parameters from the 30012, 30013, and 20012 bands of CO_2, including the line positions, the line intensities, and other line-shape parameters. They have been improved significantly with comb-assisted spectrometers in recent years [6–8]. For instance, line intensities of $^{12}C^{16}O_2$ have been determined with uncertainties below 0.1% for 30013←00001, 30012←00001, and 30014←00001 bands in the near-infrared region [9]. And the frequency accuracy of some transitions in the (30013) and (30012) bands was improved to several kHz with saturated absorption spectroscopy measurement by the groups in Grenoble [10] and Hefei [11, 12]. Their measurements covered the transitions in the P and R branches of (30013) band with J up to 72, and most lines in the P branch of the (30012) band.

This work continues our previous studies of the high precision spectrum of CO_2 by comb-locked cavity ring-down spectroscopy (CRDS) [11–13]. In this contribution, measurements were extended to the transitions of the R branch with the rotational quantum number up to 68. In experiments, the setup diagram and the spectrum retrieval methodology are presented. The frequency uncertainties and literature energy levels comparison from this work are analyzed and summarized in the results.

II. EXPERIMENTS

The comb-locked cavity ring-down spectrometer is

* Author to whom correspondence should be addressed. E-mail: awliu@ustc.edu.cn

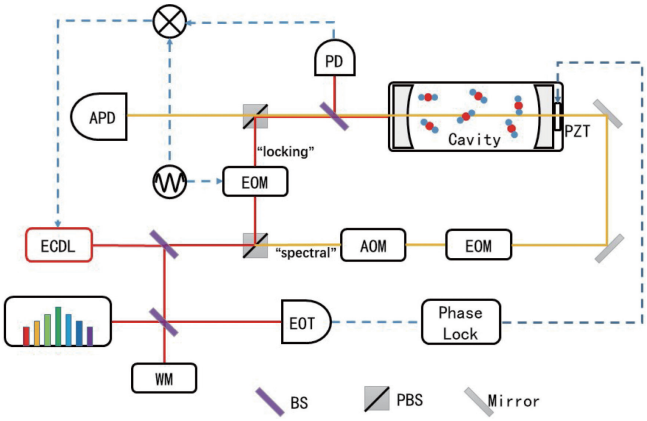

FIG. 1 Schematic diagram of the saturated cavity ring-down spectrometer. BS: beam splitter, PBS: polarized beam splitter, EOM: electronic-optic modulator, AOM: acoustic-optic modulator, WM: wavemeter, PZT: piezo actuator, APD: advalanche photodiode, PD: photodiode.

shown in FIG. 1, similar to our previous experimental setups [14, 15]. A tunable external-cavity diode laser (ECDL, Toptica DL Pro-1550) was split to the "spectral" and the "locking" beams through a polarized beam splitter (PBS). The "locking" beam was phase modulated by an electronic-optical modulator (EOM), then introduced to a ring-down (RD) cavity. The back-reflected signal from the cavity was detected by a photodiode (PD), locking the laser frequency to one longitudinal cavity mode with the Pound-Drever-Hall (PDH) method. The RD cavity is composed of a pair of high-reflectivity (HR) mirrors (R=99.997% at 1.54–1.7 μm, Layertec GmbH Inc.) with a distance of 44.6 cm, leading to a free spectral range (FSR) of 336 MHz, a finesse of 1.56×10^5. The beat signal between the laser and an optical frequency comb (OFC), which acted as a phase-lock circuit to drive a piezo actuator (PZT) and stabilized the cavity length, was monitored by an amplified photodetector (EOT-3000A). The OFC was synthesized by an Er-fiber oscillator with a repetition frequency ($f_{\rm rep}$≈184 MHz) and carrier offset frequency (f_0) referenced to a global positioning system (GPS)-disciplined rubidium clock (SRS FS725). The p-polarization "spectral" laser beam, which was shifted by an acousto-optic modulator (AOM) and a fiber-EOM, was coupled into the RD cavity and used for cavity ring-down spectroscopy measurement. When the signal measured by an avalanche photodiode (APD) reached a preset level, the AOM would shut off the laser beam and trigged a ring-down event. The nonlinear Levenberg-Marquart algorithm was applied to fit the ring-down curve to an exponential decay function. The sample absorption coefficient α was determined from the change of the cavity decay time τ according to the equation:

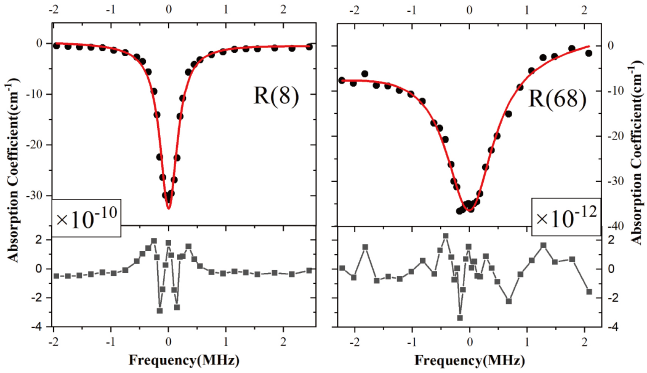

FIG. 2 Lamb-dips of the R(8) and R(68) lines in the 30012←00001 band of $^{12}C^{16}O_2$ recorded at sample pressures of 0.2 Pa and 2 Pa, respectively. Lower panels show residuals from fitting with Lorentzian profiles.

$$\alpha = (c\tau)^{-1} - (c\tau_0)^{-1}$$

here c is the speed of light, τ_0 is the decay time of the empty cavity. The minimum detectable absorption coefficient reached about 2×10^{-11} cm^{-1} with an averaging time of 1 s. The saturated absorption spectral scan was accomplished by tuning the reference frequency $f_{\rm B}$ of the phase-lock loop:

$$\nu = f_0 + N \times f_{\rm rep} + f_{\rm B} + f_{\rm AOM} + f_{\text{fiber-EOM}} \quad (1)$$

here $f_{\rm AOM}$ and $f_{\text{fiber-EOM}}$ are radio frequencies driving the AOM and fiber-EOM, respectively.

The carbon dioxide gas sample in natural abundance was bought from Nanjing Special Gas Co. with a stated purity of 99.99% and purified with a " freeze-pump-thaw" process before measurement. In this work, gas pressures ranging from 0.1 Pa to 2.0 Pa were used to obtain a high signal-to-noise level and a narrower linewidth as well. Sample pressures were measured by a manometer (CPCA-100 ShangHai ZhenTai) with a stated uncertainty of 0.5%. The measurements were performed at room temperature (296 ± 0.2 K).

III. RESULTS AND DISCUSSION

In total, 37 lines from P(4) to R(68) with the HITRAN line intensities [16] in the range of 1.46×10^{-26} to 1.76×10^{-23} cm/molecule were measured in this work. FIG. 2 shows the averaged saturated absorption spectra of the R(8) and R(68) lines recorded with sample pressures of 0.2 Pa and 2 Pa, respectively. A Lorentzian line profile with a linear baseline was used to simulate

DOI: 10.1063/1674-0068/cjcp2305046

TABLE I Frequencies of the measured transitions in the 30012←00001 band of $^{12}C^{16}O_2$.

Line	Frequency/MHz	Width (FWHM)/MHz	Depth/($\times10^{-10}$ cm^{-1})	Scans	Pressure/Pa
P4e	190 208 841.403(7)	0.41	79.7	171	0.6
P2e	190 256 762.624(7)	0.44	33.0	325	0.5
R0e	190 326 953.299(7)	0.52	22.4	387	0.6
R2e	190 372 618.525(7)	0.45	63.3	228	0.6
R4e	190 417 380.537(7)	0.39	63.3	171	0.4
R6e	190 461 239.482(7)	0.38	33.2	256	0.2
R8e	190 504 195.932(7)	0.39	34.9	223	0.2
R10e	190 546 250.897(7)	0.38	41.1	141	0.1
R12e	190 587 406.372(7)	0.36	40.4	104	0.1
R14e	190 627 660.983(7)	0.38	46.2	50	0.2
R16e	190 667 021.407(7)	0.35	47.9	103	0.2
R18e	190 705 488.038(7)	0.32	47.9	49	0.2
R20e	190 743 064.163(7)	0.32	47.7	51	0.2
R22e	190 779 753.299(7)	0.33	45.4	100	0.2
R24e	190 815 559.448(7)	0.39	44.5	51	0.2
R26e	190 850 487.010(7)	0.39	37.5	81	0.2
R28e	190 884 540.864(7)	0.29	25.2	43	0.1
R30e	190 917 726.403(7)	0.31	21.0	84	0.1
R32e	190 950 049.475(7)	0.36	18.7	56	0.1
R34e	190 981 516.452(7)	0.40	15.0	50	0.3
R36e	191 012 134.184(7)	0.40	12.1	51	0.1
R38e	191 041 910.096(7)	0.41	9.4	57	0.1
R40e	191 070 852.154(7)	0.35	8.5	37	0.2
R42e	191 098 968.892(7)	0.44	16.4	144	0.3
R44e	191 126 269.416(7)	0.58	39.7	48	1.5
R46e	191 152 763.461(7)	0.71	27.3	71	1.8
R48e	191 178 461.376(7)	0.71	18.3	55	1.8
R50e	191 203 374.162(7)	0.70	14.2	86	1.8
R52e	191 227 513.477(7)	0.66	10.1	50	1.8
R54e	191 250 891.698(7)	0.67	7.3	62	1.5
R56e	191 273 521.885(7)	0.62	4.4	100	1.5
R58e	191 295 417.866(7)	0.65	3.3	83	1.5
R60e	191 316 594.219(7)	0.72	19.0	110	1.5
R62e	191 337 066.308(7)	0.75	1.3	184	1.5
R64e	191 356 850.297(8)	0.73	1.0	122	2.0
R66e	191 375 963.208(9)	0.87	0.6	105	2.0
R68e	191 394 422.878(10)	0.87	0.3	200	2.0

the saturated absorption spectrum to retrieve the peak center, the Lamb-dip depth and width. The fitting residuals are illustrated in the lower panels of FIG. 2. Different scan numbers were applied in the measurements to achieve a signal-to-noise ratio better than 15, as seen in the fifth column of Table I. The third and fourth columns in Table I also show the FWHM-width (full width at half maximum) and the Lamb-dip depth for each line. The retrieved linewidths vary between 290 kHz and 870 kHz, which are comparable to those of the lines for $^{12}C^{16}O_2$ [11,12] and $^{12}C^{16}O$ [17] recorded under similar pressures. According to the line intensities and respectively recorded pressures, the dip depths of 37 lines range from 0.3×10^{-10} cm^{-1} to 79.7×10^{-10} cm^{-1}, with estimated saturation parameters S of 0.1–0.4 calculated with the equations given in Ref.[18].

DOI: 10.1063/1674-0068/cjcp2305046

TABLE II Uncertainty budget, 37 lines in the 30012←00001 band of $^{12}C^{16}O_2$.

Type	Source	Uncertainty/kHz
Statistics		0.1–7.0
Systematic	Frequency comb	7.0
	Cavity locking servo	0.4
	AOM and EOM	0.05
	Pressure shift	0.05–0.8
	Power shift	0.25
	Line profile asymmetry	0.5–1.5
	Second-order Doppler	0.01
Total		7.0–10.0

Note: the frequency shifts are −0.12 kHz for AOM and EOM and −0.18 kHz for second-order Doppler, respectively.

Statistic uncertainties of the line frequencies are less than 8 kHz for 37 lines. The systematic uncertainties from seven different sources were investigated, including the frequency comb, AOM and EOM, the cavity locking servo, power shift, pressure shift, line profile, and the second-order Doppler shift. Most of the systematic uncertainties are below 0.4 kHz as those discussed in our previous studies [11, 12, 15, 19]. Table II summarizes the statistic and systematic error budget. The carrier offset of the frequency comb has a long-term drift during the long-term measurement, leading to a systematic error of 7.0 kHz. Uncertainties in the driving frequencies of AOM and fiber-EOM are below 0.05 kHz. The power shift and the pressure-induced shift are measured to be within 1 kHz with the sample pressure lower than 2 Pa and the input laser power less than 2 mW, as studied by Wu *et al.* [11] and Tan *et al.* [12] for the transitions in the 30013←00001 and 30012←00001 bands. The uncertainty of the cavity locking servo is estimated to be about 0.4 kHz with the Allan deviation of the beat frequency between the probe laser and the frequency comb. The uncertainty for possible asymmetry in the line profile was estimated to be 0.5–1.5 kHz. The second-order Doppler shift, corresponding to the most probable gas velocity, is $-\nu_0 k_B T/(mc^2)$, and it gives a value of −0.18(1) kHz for $^{12}C^{16}O_2$ at room temperature. Positions of 37 lines are given in the second column of Table I together with the total uncertainties (1σ) in the range of 7.0–10.0 kHz.

Thirteen ground state combination differences ΔE_{30012} were calculated from the P(J+1) and R(J–1) line positions retrieved in Ref.[11] and this work, respectively. FIG. 3 displays the comparison of the combination difference ΔE_{30012} to ΔE_{30013} values given in the supplementary material of Ref.[12]. The difference of 83.4% in the ground state combination difference values is within the 1σ combined uncertainties, demonstrating the accuracy of the line positions determined in this work.

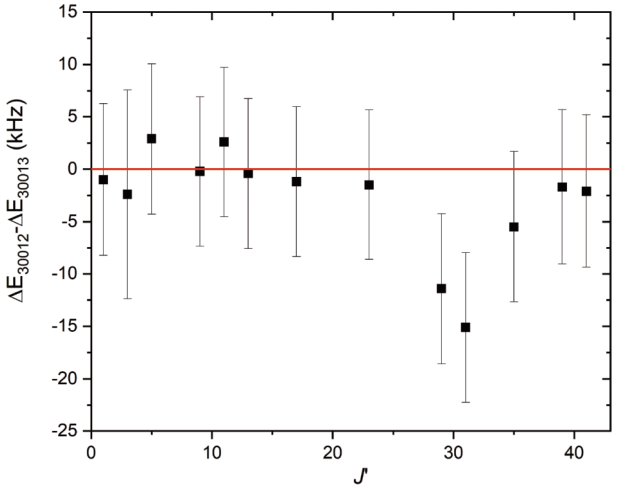

FIG. 3 Ground state combination difference ΔE_{30012} (in kHz) obtained with the P(J+1) line positions from Ref. [11] and the R(J–1) line positions determined in this work compared to ΔE_{30013} values calculated with the line pairs in Ref.[12].

In the past decade, with the development of comb-assisted cavity ring-down spectroscopy, the frequency accuracy of line positions in the 30012←00001 band of $^{12}C^{16}O_2$ have been experimentally improved to sub-MHz by Doppler-limited spectroscopy [6, 20–26]. Note that previous work mostly focused on studying the line positions in the P branch. The ground state energy levels can be obtained with accuracy better than 2 kHz using the spectroscopic parameters given in Ref.[22]. This means that we may compare results from this work with earlier studies by converting transition frequencies to rovibrational energies. Deviations of two literature results from this work are presented in the upper and middle panels of FIG. 4, where energy levels are retrieved with the experimental line positions from the NIM group [20] and the NIST group [21, 22], respectively. Deviations of more than 30% NIM's values (35 energy levels in total) are outside the 2σ combined uncertainties. The NIM group simultaneously extracted line parameters for each transition from seven spectra taken at a variety of pressures using a multi-spectrum approach. To recreate the spectrum observed at pressures ranging from 2 Torr to 95 Torr, more complicated ef-

DOI: 10.1063/1674-0068/cjcp2305046

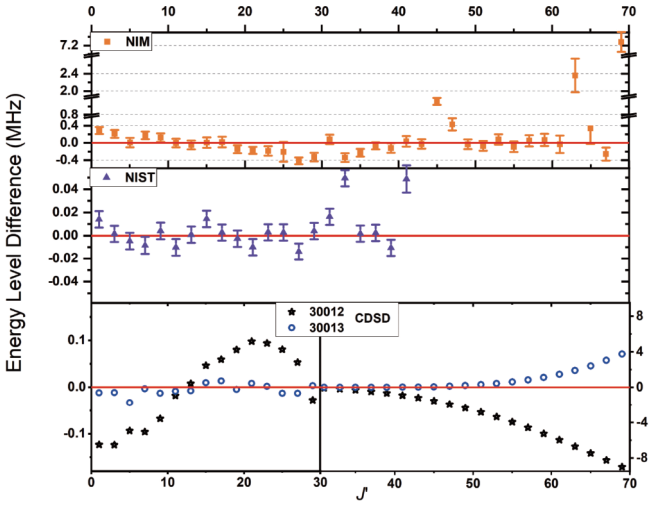

FIG. 4 Literature values difference (in MHz) from this work versus the rotational quantum number J for 35 upper ro-vibrational energy levels in the 30012←00001 band of $^{12}C^{16}O_2$. Error bars represent 1σ combined uncertainties. Data sources are energy levels retrieved with Doppler-limited experimental line positions from NIM (upper panel) [20], NIST (middle panel) [21, 22] and the carbon dioxide spectroscopic databank CDSD (lower panel, stars) [32]. Similar comparisons are also provided for values in the 30013←00001 band (lower panel, circles). In the lower panel, the left vertical axis is linked to those with $J < 30$, while the right vertical axis is related to those with $J \geq 30$.

fects such as collision narrowing and speed-dependent broadening have to be included in the line profile model. It not only increases the correlations between the line centers and other profile parameters, but also introduces systematic error in line centers when different lineshape models are used: Voigt profile (VP), Galatry profile (GP) [27], Nelkin-Ghatak profile (NGP) [28], speed-dependent VP (SDVP) [29], SDGP [30], and SDNGP [31]. It is worth noting that more than 1 MHz deviations from our values are found for energy levels of J=45 (P(46), 1.1 MHz, 14σ), J=63 (P(64), 2.4 MHz, 6σ), and J=69 (P(70), 7.3 MHz, 32σ). Some neighboring transitions of other carbon dioxide isotopologues may interfere with the frequency of $^{12}C^{16}O_2$. The deviation increases as the distance between neighboring transitions decreases. There are three transitions of $^{13}C^{16}O_2$ and $^{12}C^{16}O^{18}O$ isotopologues within a distance less than 30 MHz from the P(72) line in the 30012←0000 band of $^{12}C^{16}O_2$.

The comparison given in the middle panel of FIG. 4 includes more energy levels than the previous one given in Ref.[11]. The NIST's frequencies in Refs.[21, 22, 26] were obtained with the Doppler-limited spectrum measured at pressures with a few Pascal. Most deviations are less than 20 kHz. Note that P(34) and P(42) transitions have differences up to 49 kHz.

We also compared the rotational energy levels of 30012 and 30013 [12] vibrational states determined by our group to those archived in carbon dioxide spectroscopic databank (CDSD2019) [32], as shown in the lower panel of FIG. 4. The empirical energy levels agree well with our values for the rotational states with $J' \leq 33$ of both vibrational states. But the difference goes up to 3.8 and −9.0 MHz for 30013 and 30012 vibrational states, respectively. And the deviations have a small structure with about 0.2 MHz amplitude for J' ranging from 1 to 33 in the 30012 vibrational state. Although Tashkun *et al.* included the inter-polyad interaction between the 30012 and 33301 vibrational states in their effective Hamiltonian model, they deduced the difference by one magnitude [33]. The empirical values are better reproduced for 30013 state than 30012 state in CDSD databank, and its accuracy relies much on the experimental line positions.

IV. CONCLUSION

In conclusion, We extended the saturated absorption spectroscopy measurement of $^{12}C^{16}O_2$ lines in the 30012←00001 band to J=68 by a comb-locked cavity ring-down spectrometer near 1.57 μm. Line positions were experimentally determined with an accuracy of several kHz for 37 lines with a wide line intensity range of two orders of magnitude. The ro-vibrational energy levels of the 30012 vibrational state determined in this work were compared with those from previous Doppler-limited studies as well as those from the CDSD2019 databank. The high precision line positions can be a supplement to the frequency standards in the C band together with the results from our previous studies on CO [14, 15, 17] and CO_2 [11, 12] molecules.

V. ACKNOWLEDGMENTS

This work was jointly supported by the National Natural Science Foundation of China (No.22273093, No.41905018, and No.21903080) and the Ministry of Science and Technology of China (No.2022YFF 0606500).

[1] C. E. Miller, L. R. Brown, R. A. Toth, D. C. Benner,

and V. M. Devi, C. R. Phys. **6**, 876 (2005).
[2] H. Fleurbaey, H. Yi, E. M. Adkins, A. J. Fleisher, and J. T. Hodges, J. Quant. Spectrosc. Radiat. Transfer **252**, 107104 (2020).
[3] A. Kuze, H. Suto, M. Nakajima, and T. Hamazaki, Appl. Opt. **48**, 6716 (2009).
[4] Y. Liu, D. X. Yang, and Z. N. Cai, Chin. Sci. Bull. **58**, 1520 (2013).
[5] D. Wunch, G. C. Toon, J. Blavier, R. A. Washenfelder, J. Notholt, B. J. Connor, D. Griffith, V. Sherlock, and P. O. Wennberg, Philos. Trans. R. Soc. A **369**, 2087 (2011).
[6] D. Gatti, T. Sala, R. Gotti, L. Cocola, L. Poletto, M. Prevedelli, P. Laporta, and M. Marangoni, J. Chem. Phys. **142**, 074201 (2015).
[7] O. L. Polyansky, K. Bielska, M. Ghysels, L. Lodi, N. F. Zobov, J. T. Hodges, and J. Tennyson, Phys. Rev. Lett. **114**, 1 (2015).
[8] T. A. Odintsova, E. Fasci, L. Moretti, E. J. Zak, O. L. Polyansky, J. Tennyson, L. Gianfrani, and A. Castrillo, J. Chem. Phys. **146**, 244309 (2017).
[9] D. A. Long, Z. D. Reed, A. J. Fleisher, J. Mendonca, S. Roche, and J. T. Hodges, Geophys. Res. Lett. **47**, 2019GL086344 (2020).
[10] J. Burkart, T. Sala, D. Romanini, M. Marangoni, A. Campargue, and S. Kassi, J. Chem. Phys. **142**, 191103 (2015).
[11] H. Wu, C. L. Hu, J. Wang, Y. R. Sun, Y. Tan, A. W. Liu, and S. M. Hu, Phys. Chem. Chem. Phys. **22**, 2841 (2020).
[12] Y. Tan, Y. R. Xu, T. P. Hua, A. W. Liu, J. Wang, Y. R. Sun, and S. M. Hu, J. Chem. Phys. **156**, 044201 (2022).
[13] P. Kang, J. Wang, G. L. Liu, Y. R. Sun, Z. Y. Zhou, A. W. Liu, and S. M. Hu, J. Quant. Spectrosc. Radiat. Transfer **207**, 1 (2018).
[14] J. Wang, Y. R. Sun, L. G. Tao, A. W. Liu, T. P. Hua, F. Meng, and S. M. Hu, Rev. Sci. Instrum. **88**, 043108 (2017).
[15] J. Wang, Y. R. Sun, L. G. Tao, A. W. Liu, and S. M. Hu, J. Chem. Phys. **147**, 091103 (2017).
[16] I. Gordon, L. Rothman, R. Hargreaves, R. Hashemi, E. Karlovets, F. Skinner, E. Conway, C. Hill, R. Kochanov, Y. Tan, P. Wcisło, A. Finenko, K. Nelson, P. Bernath, M. Birk, V. Boudon, A. Campargue, K. Chance, A. Coustenis, B. Drouin, J. Flaud, R. Gamache, J. Hodges, D. Jacquemart, E. Mlawer, A. Nikitin, V. Perevalov, M. Rotger, J. Tennyson, G. Toon, H. Tran, V. Tyuterev, E. Adkins, A. Baker, A. Barbe, E. Canè, A. Császár, A. Dudaryonok, O. Egorov, A. Fleisher, H. Fleurbaey, A. Foltynowicz, T. Furtenbacher, J. Harrison, J. Hartmann, V. Hornerman, X. Huang, T. Karman, J. Karns, S. Kassi, I. Kleiner, V. Kofman, F. Kwabia–Tchana, N. Lavrentieva, T. Lee, D. Long, A. Lukashevskaya, O. Lyulin, V. Makhnev, W. Matt, S. Massie, M. Melosso, S. Mikhailenko, D. Mondelain, H. Müller, O. Naumenko, A. Perrin, O. Polyansky, E. Raddaoui, P. Raston, Z. Reed, M. Rey, C. Richard, R. Tóbiás, I. Sadiek, D. Schwenke, E. Starikova, K. Sung, F. Tamassia, S. Tashkun, J. Vander Auwera, I. Vasilenko, A. Vigasin, G. Villanueva, B. Vispoel, G. Wagner, A. Yachmenev, and S. Yurchenko, J. Quant. Spectrosc. Radiat. Transfer **277**, 107949 (2022).
[17] J. Wang, C. L. Hu, A. W. Liu, Y. R. Sun, Y. Tan, and S. M. Hu, J. Quant. Spectrosc. Radiat. Transfer **270**, 107717 (2021).
[18] C. R. Bucher, K. K. Lehmann, D. F. Plusquellic, and G. T. Fraser, Appl. Opt. **39**, 3154 (2000).
[19] J. Chen, T. P. Hua, L. G. Tao, Y. R. Sun, A. W. Liu, and S. M. Hu, J. Quant. Spectrosc. Radiat. Transfer **205**, 91 (2018).
[20] Z. D. Reed, B. J. Drouin, D. A. Long, and J. T. Hodges, J. Quant. Spectrosc. Radiat. Transfer **271**, 107681 (2021).
[21] Z. D. Reed, B. J. Drouin, and J. T. Hodges, J. Quant. Spectrosc. Radiat. Transfer **275**, 107885 (2021).
[22] R. Guo, J. Teng, H. Dong, T. Zhang, D. Li, and D. Wang, J. Quant. Spectrosc. Radiat. Transfer **264**, 107555 (2021).
[23] D. A. Long, S. Wójtewicz, C. E. Miller, and J. T. Hodges, J. Quant. Spectrosc. Radiat. Transfer **161**, 35 (2015).
[24] G. W. Truong, D. A. Long, A. Cygan, D. Lisak, R. D. Van Zee, and J. T. Hodges, J. Chem. Phys. **138**, 094201 (2013).
[25] R. Gotti, D. Gatti, P. Masłowski, M. Lamperti, M. Belmonte, P. Laporta, and M. Marangoni, J. Chem. Phys. **147**, 134201 (2017).
[26] Z. D. Reed, D. A. Long, H. Fleurbaey, and J. T. Hodges, Optica **7**, 1209 (2020).
[27] L. Galatry, Phys. Rev. **122**, 1218 (1961).
[28] M. Nelkin and A. Ghatak, Phys. Rev. **135**, A4 (1964).
[29] P. R. Berman, J. Quant. Spectrosc. Radiat. Transfer **12**, 1331 (1972).
[30] R. Ciuryło, Phys. Rev. A **58**, 1029 (1998).
[31] B. Lance, G. Blanquet, J. Walrand, and J. P. Bouanich, J. Mol. Spectrosc. **185**, 262 (1997).
[32] S. A. Tashkun, V. I. Perevalov, R. R. Gamache, and J. Lamouroux, J. Quant. Spectrosc. Radiat. Transfer **228**, 124 (2019).
[33] S. A. Tashkun, V. I. Perevalov, R. R. Gamache, and J. Lamouroux, J. Quant. Spectrosc. Radiat. Transfer **152**, 45 (2015).

DOI: 10.1063/1674-0068/cjcp2305046